濟州大學校 産業技術硏究所 論文集, 第8卷, 1號, pp.93~104, 1997. 6
Cheju National Univ. R.I.I.T. Jour., Vol.8, No.1, pp.93~104, 1997. 6

Development of a New Anisotropic Eddy Viscosity Model for the Analysis on Rod Bundle Flow Fields

Sin Kim*

봉다발 유동장 해석을 위한 새로운 비등방성 와류점성계수 모형 개발

김 신*

ABSTRACT

A computer code using the finite element method is developed to analyze the flow field in the rod bundle geometry, which are commonly met in nuclear reactors. In this code, a new model of anisotropic eddy viscosity is adopted. The representative value of the anisotropic factor is determined from the scale relation which is derived through the scale analysis methodology considering the flow pulsation phenomena. The spatial distribution is deduced qualitatively in the basis of the experimental data. The flow fields calculated by this code are compared with the experimental data and show good agreements.

Key words : Rod bundle, Flow pulsation, Anisotropic eddy viscosity

Ⅰ. Introduction

Fluid flow and heat transfer processes in rod bundles of nuclear reactors are very complicated, and basic understanding of such processes is essential to conduct fuel performance during normal operating conditions and ensure structural integrity during abnormal operations. Especially, the ultimate purpose in the design and safety analysis of nuclear reactors is to verify that DNBR (Departure from Nucleate Boiling Ratio) satisfies the safety criteria. Hence, it requires that the temperature field in fuel assemblies should be precisely analyzed and the knowledge on flow

* 제주대학교 에너지공학과
Dep. of Nuclear and Energy Eng., Cheju Nat'l Univ.

fields is indispensible to such an analysis.

In rod bundle geometry, the approach employed in simple flow analyses is often inappropriate since there are secondary flows and strong anisotropy of turbulence intensity which are not observed in simple flow through tube or parallel plates[1].

Recently, from the measurement of energy spectra, it is shown that a periodic macroscopic flow process exists between subchannels in rod bundles. Thus, such cyclic and almost periodic flow pulsations are suggested to a main process of the mixing, and some experiments were conducted to investigate the flow pulsation phenomena[2,3]. According to the experimental results, the principal frequency is known to depend on Reynolds number and the relative gap size(g/D). Assuming that this phenomenon affects the anisotropic feature of turbulent diffusion as well as the turbulent mixing between subchannels, Kim-Park[4] derived the scale relation of anisotropic factor through scale analysis methodology.

In this study, a computer code using the finite elements method is developed to analyze the turbulent flow field in rod bundles with a new anisotropic eddy viscosity model. Lam-Bremhorst low-Reynolds number $k-\varepsilon$ model[5] is used as a mathematical turbulent model. Anisotropy of turbulent diffusion is assumed to reflect flow pulsation which seems to be responsible for the turbulent mixing. The representative value of the anisotropic factor is computed from the scale relation derived by Kim-Park, and the spatial distribution is presumed from the well-known experimental data[6,7].

Steady state and axially fully developed incompressible single-phase flow fields in infinite bare rod bundles are analyzed. And this code is verified successfully by comparing the calculated flow fields with the analytic solutions and the experimental data.

II. Review of turbulence models

2.1 Anisotropic turbulent diffusion

The experimental results of eddy viscosities in rod bundle geometry show the consistency. The normal eddy viscosity is similar to that of the circular tube near the wall and is twice far from the wall[6-8]. However, the parallel one is quite different from the normal one as well as that of the tube[6,7].

Rowe et al.[9] carried out an experiment on the turbulent mixing phenomena between subchannels of rod bundles, and found the macroscopic flow near the gap, which they interpreted as the cause of the anisotropy.

Bartzis-Todreas[10] experimented on and numerically investigated the turbulent flow field in triangular-arrayed rod bundles with P/D = 1.124. They adopted the 2-equation model with anisotropy and secondary flow models, and developed a simple anisotropic model for length scales. Their results

showed that the effect of the anisotropy was greater than that of the secondary flow.

From experiments and numerical analysis, Seale[11] concluded that the secondary flow hardly contributed to the velocity and temperature profiles and the high mixing rate at the gap was caused by the anisotropy. In the gap Stanton number, St_g, the isotropic model with secondary flow produced about 13% higher mixing rates than without. However the discrepancy with the measured data was still wide. Hence, he insisted to include the anisotropic model. He assumed that the anisotropic factor, n, was a function of wall distance because n had the maximum near the wall and rapidly decreased to about 1, and chose the following distribution function after testing various functions:

$$n = 50 \exp\{-(3y/\hat{y})^2\} + 2 , \quad (1)$$

where y is normal distance from the wall and $\hat{y}$ is profile length denoting normal distance from the wall to the maximum velocity line. The calculated St_g with that function agreed with the experimental results within a 50% error.

Slagter[12] proposed a 1-equation model excluding the wall function and analyzed the turbulent flow in rod bundles neglecting the secondary flow. In this model, the anisotropic length scales with damping, which was originated from the Carajilescov-Todreas model,[13] reflected the anisotropic eddy diffusion.

Yang-Chieng[14] recommended the following anisotropic factor which had been tested by Seale[11] after they computed the flow and temperature field with various type of functions neglecting secondary flow:

$$n = 30 \exp\{-(3y/\hat{y})^2\} + 1 . \quad (2)$$

Wu[15] analyzed the turbulent flow in a trapezoidal duct with a single rod, and adopted anisotropy and secondary flow model simultaneously. The Launder-Ying model[16] was used as an algebraic stress model and the anisotropic factor was developed from the experimental data.

Recently, Kim-Park[4] performed scale analysis on the flow pulsation phenomena between rod bundle subchannels. They derived a scale relation of anisotropic factor assuming that this phenomenon plays an important role in the turbulent structure of rod bundle flow fields. In this study, this scale relation is used in developing a new anisotropic eddy viscosity model.

2.2 Low-Reynolds number model

Most of the turbulence models are devised for high Reynolds number and fully turbulent flows far from the wall. Thus the success of the prediction of wall-bounded shear flows depends, to a large extent, on the use of the appropriate wall functions that relate surface boundary conditions imposed on points in the fluid away from the boundaries and thereby avoid the problem of modeling the direct influence

of viscosity. However, in some cases such as subchannel analysis where the ultimate purpose is to find the rod surface temperature and information on the flow field in the immediate vicinity of the wall is essential, the low-Reynolds number model is required.

Many low-Reynolds number models combined with widely used $k-\varepsilon$ model were proposed[17]; Lam-Bremhorst model and Launder-Sharma model are the most successful in using this approach. Especially, the Lam-Bremhorst model has the advantage in that it does not require additional terms to the standard $k-\varepsilon$ model.

III. Modelling of anisotropic eddy viscosity

Kim-Park's representative value of anisotropic factor[4] is expressed in terms of geometric factors and Strouhal number of flow pulsation in rod bundles:

$$\overline{n} = \frac{1 + 2a_x b \dfrac{(z_{FP}/D)(\delta/D)}{g/D} Str}{1 + 2a_y (z_{FP}/D)\, Str} . \tag{3}$$

In this, D, δ and g are rod diameter, centroid-to-centroid distance and gap size respectively. The z_{FP} is the path length of hypothetical flow which is assumed to represent the flow pulsation phenomenon and is approximated as

$$\frac{z_{FP}}{D} \sim \frac{\pi}{\sqrt{2}} \sqrt{b^2 \left(\frac{\delta}{D}\right)^2 + \left(\frac{g}{D}\right)^2} . \tag{4}$$

The shape factor, b, is introduced to reflect the effect of obstacles which may be located in the front of the flow pulsation. For an open path such as in the square-arrayed rod bundle and the rod-wall gap of a wall-bounded subchannel, $b = 1.0$. And $b = 2/3$ is recommended for a blocked path such as in the triangular-arrayed rod bundle and in the rod-rod gap of a wall- bounded subchannel. Velocity coefficients a_x and a_y, which are functions of geometric factors only, are approximated as

$$\begin{aligned} a_x &= 1.0 - 0.15\left(\frac{g}{D}\right) , \\ a_y &= 0.36\left(\frac{g}{D}\right) . \end{aligned} \tag{5}$$

And they recommended that Wu-Trupp's Strouhal number correlation[3] should be used in conjunction with the scale relation. The correlation is

$$Str^{-1} = 0.822\left(\frac{g}{D}\right) + 0.144 . \tag{6}$$

Before the above scale relation of the anisotropic factor derived by Kim-Park is used to reflect the anisotropy of turbulent diffusion in numerical analysis, some modification should precede because the anisotropic factor is not a constant over the flow field. Actually it depends on the location[6,7], so that the representative value, $\overline{n}$, of the factor should be modified. The spatial distribution is assumed as

$$\ln(n(r,\theta)) = f_\theta(\theta) \ln(f_r(r)) \tag{7}$$

because Rehme's experimental data shows that the parallel component of the eddy viscosity decreases exponentially as the angle from the gap. The profiles for each direction should be modelled.

Rehme's data also shows that the variation of normal components as wall distance is similar to that of the error function:

$$f_r(r) = A\,\bar{n}\exp(-a y^2) + 1 , \quad (8)$$

where a is a constant to be determined and A is the normalization constant which makes $\bar{n}$ average value. Seale[11] and Yang-Chieng[14] proposed that the error function type profile of the anisotropic factor is appropriate after testing various types of profile functions. And, it is assumed that the anisotropy disappears at the maximum angle from the gap, $\theta = \theta_{max}$. Then,

$$f_\theta(\theta) = 1 - \frac{\theta}{\theta_{max}} . \quad (9)$$

Thus, in this work, the final form of the spatial-dependent anisotropic factor is given as,

$$n(r,\theta) = \left[\frac{6\bar{n}}{\sqrt{\pi}}\exp\left\{-\left(\frac{6y}{D_H}\right)^2\right\} + 1\right]^{(1-\theta/\theta_{max})} , \quad (10)$$

where $6/\sqrt{\pi}$ is the normalization constant stated above.

Comparing the newly-developed anisotropic factor and those of Seale and Yang-Chieng, there are some different points. At first, the magnitude of anisotropy is obtained from the interpretation on the flow pulsation, which depends on the geometry. Actually the parallel eddy viscosity is closely related to g/D[18]. And damping of the factor in the azimuthal direction is considered. Experiments show that the factor decreases as the angle from the gap increases[6,7]. Finally, the normal distance was normalized not by the profile length, $\hat{y}$, but by hydraulic radius, $D_H/2$, which is a typical length scale of non-circular duct. Although Seale and Yang-Chieng regarded the anisotropic factor as a constant on the maximum velocity line, there is no evidence that the anisotropy disappears or has a constant magnitude there[6,7]. It is more reasonable to presume that near the gap the anisotropy exists even on the maximum velocity line.

IV. Numerical analysis

4.1 Mathematical models

The velocity distributions are predicted through the numerical analysis on the flow field in rod bundles. As a turbulence model, Lam-Bremhorst low-Reynolds number $k-\varepsilon$ model[5] is used. No slip wall boundary condition is adopted in place of the wall function because the ultimate purpose of the thermal hydraulic analysis on the nuclear rod bundles is to find the wall temperature.

Also, the anisotropic turbulent diffusion model developed in this study

is included in order to investigate the flow field realistically. The flow is assumed to be steady state and axially fully developed. And the secondary flow is neglected because it has only a marginal effect on the flow field as mentioned above.

4.1.1 Governing Equaticns

The governing equations for the analysis of the flow field in subchannels are established as follows and, for simplicity, the Cartesian tensor notations are used: the subscripts i and j denote lateral coordinates 1(normal to the wall) and 2(parallel to the wall), respectively.

· Axial momentum equation

$$-\frac{\partial}{\partial x_i}\left((\nu\delta_{ij}+\nu_{ij})\frac{\partial U_3}{\partial x_j}\right) = -\frac{1}{\rho}\frac{\partial p}{\partial x_3} \tag{11}$$

· Turbulent kinetic energy equation (k equation)

$$-\frac{\partial}{\partial x_i}\left((\nu\delta_{ij}+\nu_{ij}/\sigma_k)\frac{\partial k}{\partial x_j}\right) = P_k-\varepsilon\,, \tag{12}$$

$$P_k = -\overline{u_1u_3}\frac{\partial U_3}{\partial x_1} - \overline{u_2u_3}\frac{\partial U_3}{\partial x_2}\,, \tag{13}$$

where $\sigma_k = 1.0$

· Turbulent kinetic energy dissipation rate equation (ε equation)

$$-\frac{\partial}{\partial x_i}\left((\nu\delta_{ij}+\nu_{ij}/\sigma_\varepsilon)\frac{\partial \varepsilon}{\partial x_j}\right) = C_{\varepsilon 1}f_{\varepsilon 1}\frac{\varepsilon}{k}P_k - C_{\varepsilon 2}f_{\varepsilon 2}\frac{\varepsilon^2}{k}\,, \tag{14}$$

where $\sigma_\varepsilon = 1.3$, $C_{\varepsilon 1} = 1.44$ and $C_{\varepsilon 2} = 1.92$

· Anisotropic eddy viscosity model

$$-\overline{u_iu_3} = \nu_{ij}\frac{\partial U_3}{\partial x_j} \quad (for\ i\neq j,\ \nu_{ij}=0) \tag{15}$$

$$\nu_{11} = C_\mu f_\mu\frac{k^2}{\varepsilon}\,,\quad \nu_{22} = n\nu_{11} \tag{16}$$

where $C_\mu = 0.09$

· Lam-Bremhorst damping model

$$f_\mu = (1-\exp(-B_\mu R))^2\left(1+\frac{D_\mu}{R_t}\right)\,, \tag{17}$$

$$f_{\varepsilon 1} = 1+\left(\frac{A_{\varepsilon 1}}{f_\mu}\right)^3\,,\quad f_{\varepsilon 2} = 1-\exp(-R_t^2) \tag{18}$$

$$R = \frac{k^{1/2}x_l}{\nu}\,,\quad R_t = \frac{k^2}{\varepsilon\nu} \tag{19}$$

where $B_\mu = 0.0165$, $D_\mu = 20.5$ and $A_{\varepsilon 1} = 0.05$

4.1.2 Boundary Conditions

The boundaries of the subject domain consist of rod surface and symmetry boundary as shown in Fig. 1. Thus, two types of boundary conditions are needed: no-slip condition on the rod surface and symmetry condition on the symmetry boundary.

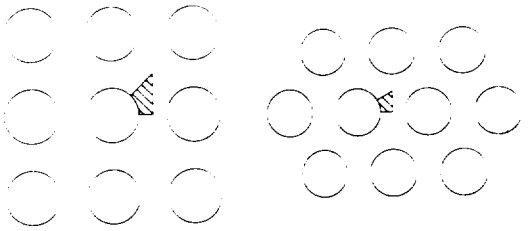

(a) Square array (b) Triangular array

Fig. 1 Schematic of rod bundle geometries

On the rod surface, all components of the velocities and turbulent kinetic energy are zero from the no-slip condition. However, for dissipation rate of turbulent kinetic energy, the boundary condition is neither exact nor simple. Furthermore, some of them, even used commonly, are likely to cause the divergence of solutions especially at high Reynolds number[19]. Thus, in this study, a new type of wall condition of third order[20] is adopted, with the Taylor expansion and the near wall behavior of turbulence under the assumption that the length of the first and the second grid are equal, as follows:

$$\varepsilon_w = \frac{3k_{w+1}}{k_{w+2} - k_{w+1}} \varepsilon_{w+1} . \qquad (20)$$

On the symmetry boundaries, the normal gradients of axial velocity, turbulent kinetic energy and its dissipation rate are set to zero.

4.2 Numerical Scheme

The governing equations are formulated numerically by the Galerkin weighted residual finite element method using bilinear and linear cardinal bases satisfying the C^0 continuity. The two dimensional calculation domain is discretized into square and triangular finite elements.

In general, numerical analyses on turbulent flows suffer from severe non-linearity and numerical instability. Thus, the initial guesses of dependent variables, mesh spacing and iteration scheme must be determined carefully. Initial profiles of the axial velocity, turbulent kinetic energy and its dissipation rate are obtained by universal profiles[21-23]. The universal velocity profile is also used to determine the mesh spacing. To filter the oscillatory behavior of numerical solutions, the guessed values for the next iteration are obtained by using the geometric mean of the value of the previous iteration step and the calculated value with an under-relaxation factor.

The convergence criteria used is that the maximum individual relative error should be below 10^{-3}. All of the governing equations are not solved simultaneously, but segregatedly.

V. Results and discussion

The calculations of the flow field in the domains shown in Fig. 1 are implemented using the turbulent model described above. In order to validate the code, the predicted distributions of axial velocities under various geometrical and hydraulic conditions are compared with

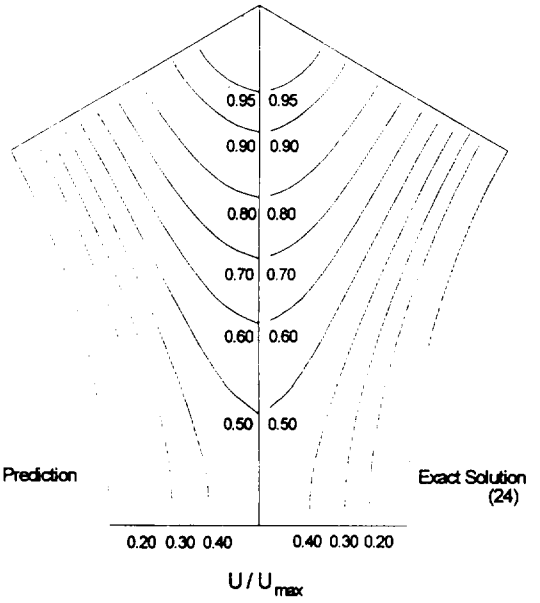

Fig. 2 Predicted and exact velocity contours for laminar flow in a triangular array(P/D = 1.20)

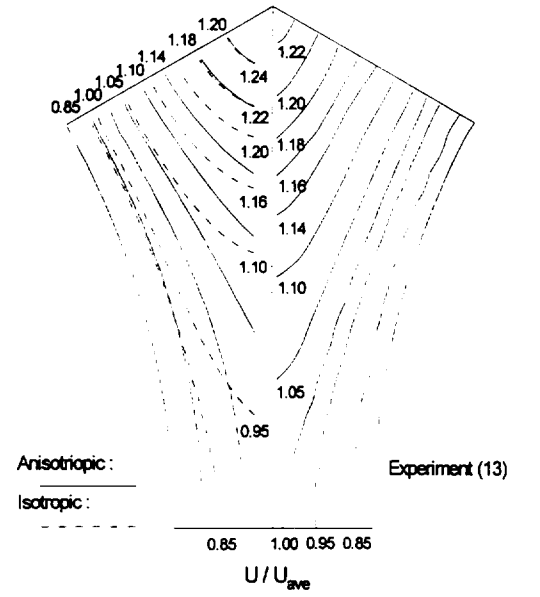

Fig. 3 Axial velocity contour in a triangular array (P/D = 1.123, Re = 27,000)

analytic solution or well-known experimental data.

Sparrow-Loeffler[24] found the exact solution of axial velocity for the fully developed laminar flow through the rod bundles. Fig. 2 shows an excellent agreement between the prediction in this study and the exact solution.

Fig. 3 shows the comparison of the computed axial velocity contours with the experimental results on a triangular array[13] of P/D = 1.123 and Re = 27,000. The anisotropy makes flow fields uniform. The predictions with the anisotropy of eddy viscosity reproduce the experimental results sufficiently well.

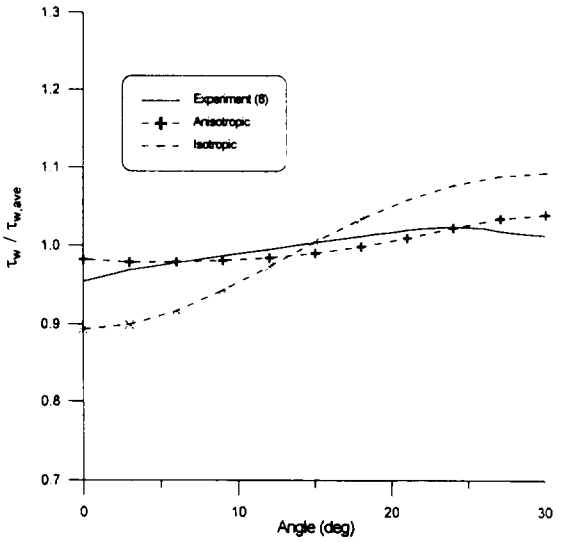

Fig. 4 Wall shear stress variation in a triangular array (P/D = 1.20, Re = 49,000)

To verify the predictability of wall shear stress, the experimental result of Trupp-Azad[8] is compared in Fig. 4. Analogously to the axial velocity profile

prediction, without the anisotropic model, the prediction fails to predict the experimental results.

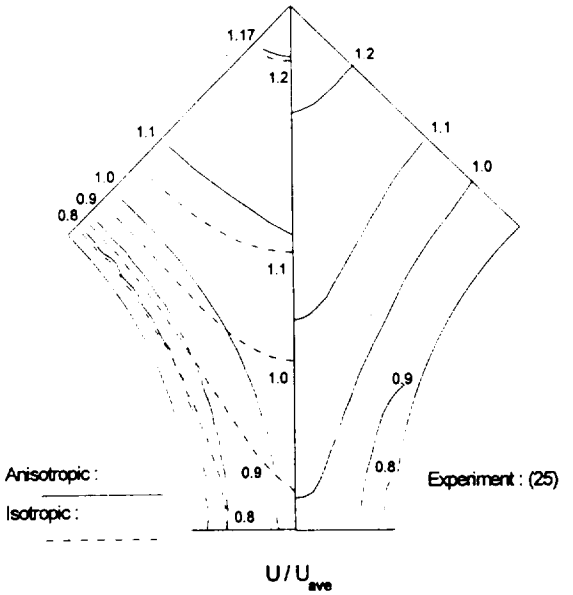

Fig. 5 Axial velocity contour in a square array (P/D = 1.25, Re = 100,000)

The comparison with the experimental data of Rowe[25] in square arrayed rod bundles is shown in Fig. 5 and it is less satisfactory than that in the triangular array. However, taking into account the experimental error of ± 3.2%, the relative error of 5% is reasonable.

Ⅵ. Conclusion

A flow field analysis code is developed using the finite element method to investigate turbulent flow field in rod bundles. Lam-Bremhorst low-Reynolds number $k-\varepsilon$ model[5] is adopted as a turbulent model and a newly-developed anisotropic eddy viscosity model is included to reflect the anisotropic diffusion characteristics of the turbulent flow field in rod bundles. The representative value of the anisotropic factor is determined from Kim-Park's scale relation[4] based on the interpretation on flow pulsation phenomena and the distribution function is constructed on the basis of the qualitative behavior of eddy viscosities shown in Rehme's experimental data[6,7].

Comparisons of numerical results and experimental data establish the usefulness of the newly-developed anisotropic eddy viscosity model. And numerical analyses without consideration of anisotropy of turbulent diffusion fail to reproduce the experiments.

Ⅶ. 요 약

원자로에서 흔히 부딪히게 되는 봉다발 구조에서의 유동장을 해석하기 위하여 유한요소법을 사용한 전산 코드를 개발하였다. 이 코드에는 새로운 비등방성 와류점성계수 모형이 도입되었다. 비등방성 인자의 대표 값은 유동맥동현상에 대한 고찰을 통해 척도 평가한 척도 상관식으로부터 얻었으며, 공간 분포는 알려진 실험자료에 기초하여 정성적으로 결정하였다. 이 모형으로 계산한 유동장을 실험 자료와 비교한 결과 잘 일치하는 것으로 나타났다.

NOMENCLATURE

a_x, a_y	velocity coefficients
$A_{\varepsilon 1}$	turbulent model constant

b	shape factor
B_μ, $C_{\varepsilon 1}$, $C_{\varepsilon 2}$, C_μ	turbulent model constants
D	rod diameter
D_H	hydraulic diameter
D_μ	turbulent model constants
f_r, f_θ	spatial distribution function of anisotropic factor for r and θ direction
$f_{\varepsilon 1}$, $f_{\varepsilon 2}$, f_μ	damping factors used in Lam-Bremhorst low-Reynolds number $k-\varepsilon$ model
g	gap size
k	turbulent kinetic energy
n	anisotropic factor
p	pressure
P_k	turbulent kinetic energy production rate
r	radial coordinate
Re	Reynolds number based on hydraulic diameter
St_g	gap Stanton number
Str	Strouhal number
U_i	mean velocity of I direction
$\overline{u_i u_j}$	Reynolds stress
x_i	coordinate of i direction
y	normal distance from the wall
$\hat{y}$	profile length
z_{FP}	hypothetical path length of flow pulsation

Greek

δ	centroid-to-centroid distance
δ_{ij}	Kronecker delta
ε	dissipation rate of turbulent kinetic energy
θ	azimuthal coordinate
ν	molecular kinematic viscosity
ν_{ij}	anisotropic eddy viscosity
ρ	density
σ_k, σ_ε	Prandtl number for turbulent kinetic energy and its dissipation rate
τ_w	wall shear stress

Subscript

i, j	Cartesian index (1 for normal to the wall, 2 for parallel to the wall, 3 for axial direction)

Symbol

overbar	representative value

REFERENCES

1) Hooper, J. D., 1980, Development Single Phase Turbulent Flow through a Square-Pitch Rod Cluster, Nucl. Eng. Des., Vol. 60, pp. 365-379.

2) Möller, S. V., 1992, Single-Phase Turbulent Mixing in Rod Bundles, Exp. Thermal Fluid Sci., Vol. 5, pp. 26-33.

3) Wu, X., and Trupp, A. C., 1994, Spectral Measurements and Mixing Correlation in Simulated Rod Bundle,

Int. J. Heat Mass Transfer, Vol. 37, pp. 1277-1281.

4) Kim, S. and Park, G.-C., 1997, Estimation of Anisotropic Factor and Turbulent Mixing Rate in Rod Bundles Based on Flow Pulsation Phenomenon, Nucl. Tech., Vol. 117, pp. 340-352.

5) Lam, C. K. G. and Bremhorst, K., 1981, A Modified Form of the $k-\varepsilon$ Model for Predicting Wall Turbulence, J. Fluids Eng., Vol. 103, pp. 456-460.

6) Rehme, K., 1978, The Structure of Turbulent Flow through a Wall Subchannel of a Rod Bundle, Nucl. Eng. Des., Vol. 45, pp. 311-323.

7) Rehme, K., 1987, The Structure of Turbulent Flow through Rod Bundles, Nucl. Eng. Des., Vol. 99, pp. 141-154.

8) Trupp, A. C. and Azad, R. S., 1975, The Structure of Turbulent Flow in Triangular Array Rod Bundles, Nucl. Eng. Des., Vol. 32., pp. 47-84.

9) Rowe, D. S., Johnson, B. M. and Knudsen, J. G., 1974, Implications Concerning Rod Bundle Crossflow Mixing Based on Measurements of Turbulent Flow Structure, Int. J. Heat Mass Transfer, Vol. 17, pp. 407-419.

10) Bartzis, J. G. and Todreas, N. E., 1979, Turbulence Modeling of Axial Flow in a Bare Rod Bundle, J. Heat Transfer, Vol. 101, pp. 628-634.

11) Seale, W. J., 1979, Turbulent Diffusion of Heat between Connected Flow Passages, Part II: Predictions Using the '$k-\varepsilon$' Turbulence Model, Nucl. Eng. Des., Vol. 54., pp. 197-209.

12) Slagter, W., 1982, Finite Element Solution of Axial Turbulent Flow in a Bare Rod Bundle Using One-Equation Turbulence Model, Nucl. Sci. Eng., Vol. 82, pp. 243-259.

13) Carajilescov, P. and Todreas, N. E., 1976, Experimental and Analytical Study of Axial Turbulent Flows in an Interior Subchannel of Bare Rod Bundle, J. Heat Transfer, Vol. 98, pp. 262-268.

14) Yang, A.-C. and Chieng, C.-C., 1987, Turbulent Heat and Momentum Transports in an Infinite Rod Array, J. Heat Transfer, Vol. 109, pp. 599-605.

15) Wu, X., 1994, Numerical Study on the Turbulence Structures in Closely Spaced Rod Bundle Subchannels, Num. Heat Transfer, Vol. 25, pp. 649-670.

16) Launder, B. E. and Ying, W. M., 1973, Prediction of Flow and Heat Transfer in Ducts Square Cross-section, Proc. Instn Mech. Engrs, Vol. 187, pp. 455-461.

17) Patel, V. C., Rodi, W. and Scheuerer, G., 1984, Turbulence Models for Near-Wall and Low Reynolds Number Flow : A Review, AIAA J. Vol. 23, pp. 1308-1319.

18) Rehme, K., 1992, The Structure of Turbulence in Rod Bundles and the Implications on Natural Mixing between the Subchannels, Int. J. Heat Mass Transfer, Vol. 35, pp. 567-581.

19) Roache, P. J., 1972, *Computational Fluid Dynamics*, Hermosa Publisher, Albuquerque, New Mexico, pp. 140-146.

20) Kim, S. and Park, G.-C., 1995, Numerical Determination of Lateral Loss Coefficients for Subchannel

Analysis in Nuclear Fuel Bundles, Proc. NUTERH-7 (NUREG/CP-0142 Vol. 4), pp. 2773-2784.

21) Tennekes, H. and Lumley, J. L., 1973, *A First Course in Turbulence*, The MIT Press, Cambridge, Massachusetts, pp. 149-165.

22) Seale, W. J., 1982, Measurements and Predictions of Fully Developed Turbulent Flow in a Simulated Rod Bundle, J. Fluid Mech., Vol. 123, pp. 399-423.

23) Jaeger, M. and Dhatt, G., 1992, An Extended $k-\varepsilon$ Finite Element Model, Int. J. Numer. Meth. Fluids, Vol. 14, pp. 1325-1345.

24) Sparrow, E. M. and Loeffler, A. L., 1959, Longitudinal Laminar Flow between Cylinders Arranged in Regular Array, A.I.Ch.E. J., Vol. 5, pp. 325-330.

25) Rowe, D. S., 1973, Measurement of Turbulent Velocity Intensity and Scale in Rod Bundle Flow Channels, BNWL-1736, Battelle Pacific Northwest Laboratories.